

Dielectric Properties of Ferroelectric Liquid Crystals with Diversified Molecular Structure

J.M. CZERWIEC^{a,*}, R. DAŁBROWSKI^b, M. ŻUROWSKA^b, D. ZIOBRO^{b,†} AND S. WRÓBEL^a

^aInstitute of Physics, Jagiellonian University, Reymonta 4, 30-059 Cracow, Poland

^bInstitute of Chemistry, Military University of Technology, S. Kaliskiego 2, 00-908 Warsaw, Poland

Mesomorphic, thermodynamic, electro-optic and dielectric properties of three homologues of fluorosubstituted esters are described. Full chemical names of these compounds are as follows: (S)-(+)-4-(1-methylheptyloksy)benzoate-(6-pentafluoropropanoynloxyhex-1-oxy)-biphenyl-4-yl (in short 2F6BBiOC8), (S)-(+)-4-(1-methylheptyloksy)benzoate-(6-nonafluoropentanoynloxyhex-1-oxy)-biphenyl-4-yl (in short 4F6BBiOC8), (S)-(+)-4-(1-methylheptyloksy)benzoate-(6-tridecafluoroheptanoynloxyhex-1-oxy)-biphenyl-4-yl (in short 6F6BBiOC8). The compounds exhibit ferroelectric smectic C* phase between crystalline and isotropic phase. Only one compound (6F6BBiOC8) shows antiferroelectric phase (SmC_A^{*}) observed by dielectric spectroscopy, but the range of this phase is narrow of about 2°. All three compounds exhibit in the SmC* phase Goldstone mode and Maxwell–Wagner relaxation hidden in the conductivity contribution at low frequencies, whereas in the SmC_A^{*} phase two antiferroelectric modes (AFM1) and (AFM2) contribute to the dielectric spectrum. The compounds were studied using differential scanning calorimetric, frequency domain dielectric spectroscopy, and reversal currents method to determine spontaneous polarization.

PACS numbers: 77.84.Nh, 78.15.+e, 64.70.M–

1. Introduction

Calorimetric, dielectric and electro-optic studies of chiral liquid crystalline compounds of the series of fluorosubstituted esters, showing ferroelectric and antiferroelectric phase, have been done. Conclusions about the influence of fluorinated chain length on the presence and width of each phase during heating and cooling will be presented. The nature of Goldstone mode and Maxwell–Wagner relaxation in the SmC* phase and two anti-ferroelectric modes (AFM1) and (AFM2) in the anti-ferroelectric SmC_A^{*} phase will also be discussed.

All three compounds are homologues of fluoro-substituted esters with three phenyl rings (in short *n*F6BBiOC8). The measurements were done for *n* = 2 and 4 and 6, where *n* is the number of carbons in the end chain. Their molecular structures are presented in Fig. 1.

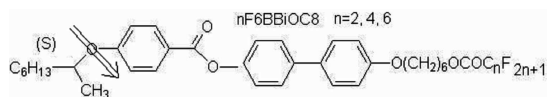


Fig. 1. Molecular structures of *n*F6BBiOC8, fluoro-substituted esters having three rings in molecular core.

* corresponding author; e-mail: jan.czerwiec@uj.edu.pl

† This Author was erroneously omitted in printed version of the paper. J.M.C. would like to apologize this error.

The substances studied were synthesized in the Institute of Chemistry of the Military University of Technology. They belong to a class of orthoconic liquid crystals [1] applicable in high contrast liquid crystal displays (LCDs). All substances studied exhibit ferroelectric SmC* phase in wide temperature range. They are good candidates for room temperature ferroelectric mixtures [2]. It is interesting that all these substances exhibit a direct transition from the isotropic to ferroelectric SmC* phase.

2. Experimental

DSC measurements were done by using differential scanning calorimeter — Pyris 1 DSC. Substances were put into the aluminum crucibles and sealed by the crimper press. The mass of samples studied was between 4.5 and 4.8 mg.

Electro-optic and dielectric measurements were done using 5.3 μm planar cells. Measurements have been done using thin layer monodomains grown in a strong electric field applied upon cooling from the isotropic to ferroelectric phase. Examples of textures are presented in Fig. 2. Textures in Fig. 2a and Fig. 2b present partial alignment in electric field. Due to AC field the alignment of SmC* phase is improving (Fig. 2b). Figure 2c presents the texture of a partially aligned SmC_A^{*} of 6F6BBiOC8.

Electro-optic measurements were done using glass cells with indium tin oxide electrodes (ITO-HG). Polarizing microscope Jenapol equipped with Instec HCS410 hot stage was employed for texture observation. *P_s* was

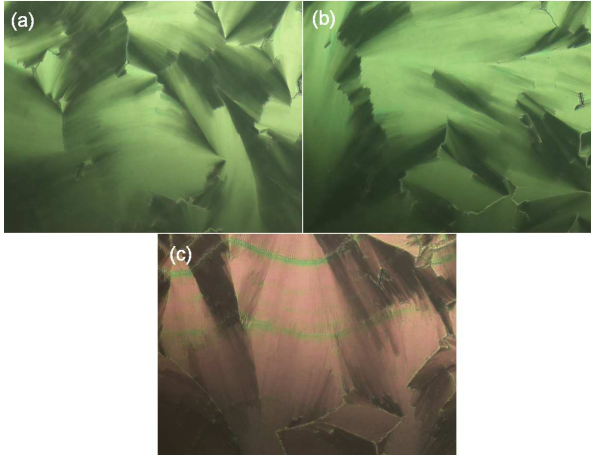


Fig. 2. (a) Influence of electric field ($U = 100 V_{p-p}$, $\nu = 100$ Hz) on the texture of SmC^* phase close to the I- SmC^* transition ($T = 135$ °C), (b) Texture of the SmC^* observed after longer exposition to AC field ($T = 135$ °C). (c) Texture of partially aligned SmC_A^* phase of 6F6BBiOC8 ($T = 65$ °C).

measured versus temperature on partially aligned samples (planar inhomogeneous) by reversal currents method (RCM) at different frequencies of the driving triangular wave. To this end an Agilent 33120A waveform generator and a F20ADI voltage amplifier and Sony CCD camera have been used.

Dielectric measurements were performed with the use of frequency domain dielectric spectroscopy (FDDS) method using Agilent 4294A impedance analyzer connected to gold planar cells (Au-HG) filled with liquid crystalline material above the clearing temperature. At a given temperature, four hundred experimental points were obtained in the frequency range between 40 Hz and 10 MHz. Temperature was controlled by Eurotherm 2604. The value of measuring voltage was equal to $0.1 V_{RMS}$. Agilent 4294A registers: the capacity and loss factor $\tan \delta$, and conductivity of the sample at each frequency. Special software is used to calculate the complex dielectric permittivity.

3. Results and discussion

3.1. Phase behavior

DSC and electro-optic measurements show that all compounds studied exhibit a direct transition from the isotropic to ferroelectric phase. Their DSC plots are presented in Fig. 3. Only for 6F6BBiOC8 there is an anti-ferroelectric phase (SmC_A^*) below the ferroelectric phase (SmC^*) as it is shown in Fig. 3 and Table I. Few scans from crystal to isotropic and back with different scan rates: 10, 20 and 40 deg/min show that the temperature stability of the each compound is high. All DSC measurements were done for similar masses of the samples — between 4.5 and 4.8 mg.

TABLE I

Temperature ranges of SmC^* phase for three compounds studied by DSC.

Acronym/run	Heating	Cooling
2F6BBiOC8	Cr 61 °C SmC^* 125 °C I	I 122 °C SmC^* 51 °C SmC_A^* 37 °C Cr
4F6BBiOC8	Cr 61 °C SmC^* 131 °C I	I 127 °C SmC^* 54 °C SmC_A^* 44.5 °C Cr
6F6BBiOC8	Cr ₁ 60 °C Cr ₂ 70.8 °C SmC^* 142.7 °C I	I 127 °C SmC^* 58 °C SmC_A^* 44.5 °C Cr

As seen from Table I all these compounds display in the low temperature range the antiferroelectric phase. For 6F6BBiOC8 it was disclosed by texture observation and dielectric spectroscopy.

3.2. Spontaneous polarization

Spontaneous polarization was computed by using the formula (1),

$$P_s = \frac{1}{R} \frac{A}{2S}, \quad (1)$$

where R is the resistance of the resistor being in series

with the electro-optic cell, A is the area under the response current spectrum, S is the surface of ITO electrodes. P_s vs. temperature plots are depicted in Fig. 4 for all compounds studied.

As it is presented in Fig. 4, P_s does not depend strongly on the chain length. Maximum value of P_s is around 50 nC/cm². Small values of spontaneous polarization are due to molecular structure of compounds studied [3, 4]. Permanent dipole moment of polar group (C–O–C) being close to the chiral center is small ($\mu = 0.7$ D).

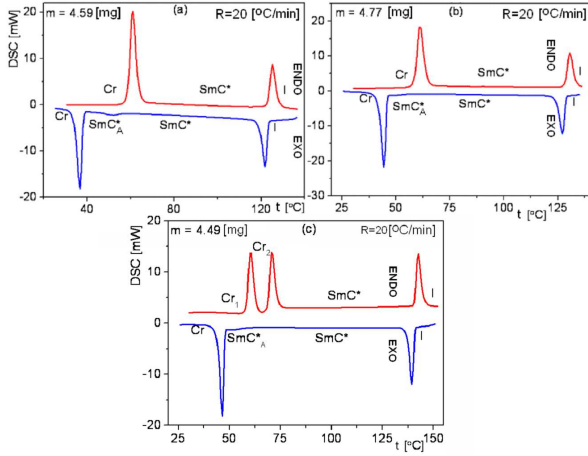


Fig. 3. DSC ENDO and EXO plots for (a) 2F6BBiOC8, (b) 4F6BBiOC8, and (c) 6F6BBiOC8.

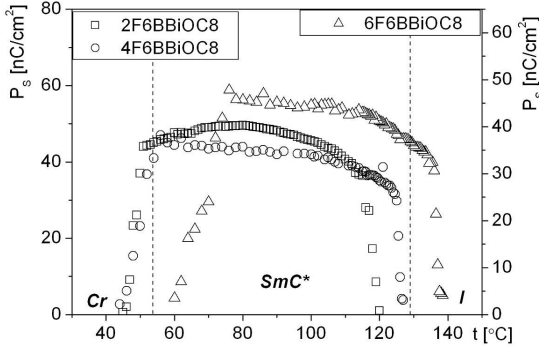


Fig. 4. Spontaneous polarization of SmC* phases as a function of temperature for n F6BBiOC8.

3.3. Dielectric study

Dielectric spectra were measured on cooling of the samples. A Cole–Cole function Eq. (2) with conductivity term and with two relaxation processes for SmC* phase and SmC_A* was fitted to the experimental data,

$$\varepsilon_{\perp}^*(\nu) = \varepsilon'_{\perp} - i\varepsilon''_{\perp} = \varepsilon_{\perp}(\infty) + \sum_{k=1}^2 \frac{\Delta\varepsilon_{\perp k}}{1 + \left(i \frac{\nu}{\nu_{Rk}}\right)^{1-\alpha_k}} - i \frac{\sigma}{\varepsilon_0 2\pi\nu}, \quad (2a)$$

$$\tau_{Rk} = \frac{1}{2\pi\nu_{Rk}}, \quad (2b)$$

$$\Delta\varepsilon_{\perp k} = \varepsilon_{\perp}(0) - \varepsilon_{\perp}(\infty), \quad (2c)$$

where ν is frequency of measuring electric field, τ_R — dielectric relaxation time, $\varepsilon_{\perp}(\infty)$ — electric permittivity in high frequency range, $\varepsilon_{\perp}(0)$ — static electric permittivity, ε_0 — electric permittivity of free space, α — distribution parameter of relaxation time and $\sigma(\nu)$ — ionic conductivity. All these parameters were computed by fitting Eq. (2) to the experimental data.

Figure 5 presents dielectric dispersion and absorption vs. frequency and Cole–Cole diagram of 6F6BBiOC8 for the SmC* and SmC_A* phases.

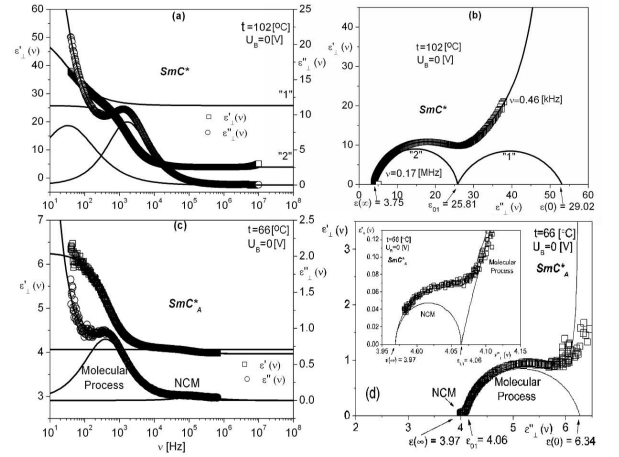


Fig. 5. Dielectric dispersion and absorption of SmC* (a) and SmC_A* (c) of 6F6BBiOC8. Cole–Cole diagram of SmC* (b) and SmC_A* (d) of 6F6BBiOC8. “1” is a Maxwell–Wagner relaxation (MW) and “2” is a Goldstone mode (GM). Inset drawing in part (d) depicts AFM2.

As it is presented in Fig. 5 and Table II, there are two relaxation processes in the SmC*, namely Maxwell–Wagner relaxation (MW) in the low frequency range and Goldstone mode (GM) at higher frequencies. MW relaxation is overwhelmed by conductivity contribution and it can be extracted from the experimental data by using Eq. (2) for fitting procedure. $\Delta\varepsilon$ values of both processes are similar, and close to 25. One should point out that the conductivity of the antiferroelectric phase: $\sigma_{AF} = 2.6 \times 10^{-9}$ S/m is by two orders of magnitude smaller than that of ferroelectric SmC* phase ($\sigma_F = 2.6 \times 10^{-7}$ S/m).

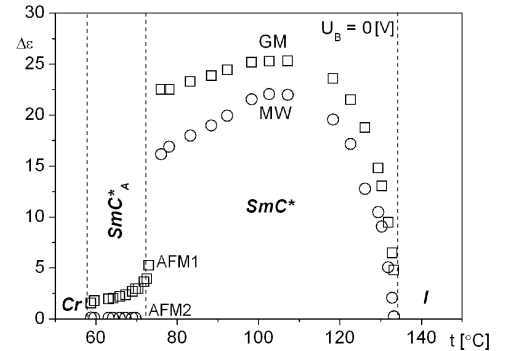


Fig. 6. Dielectric increment vs. temperature for different process of 6F6BBiOC8.

In the SmC_A* there are also two relaxation processes [5] contributing to the dielectric spectrum: antiferroelectric mode 1 (AFM1) at low frequencies and antiferroelectric mode 2 (AFM2) at higher frequencies. The dielectric increment ($\Delta\varepsilon$) of AFM2 is much lower than that for AFM1 (Table II). Temperature dependences of the dielectric increment are shown in Fig. 6. As seen in the

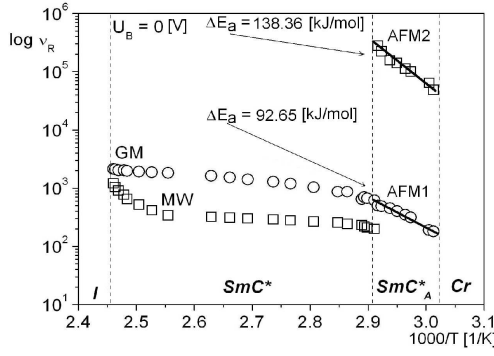


Fig. 7. Relaxation frequencies vs. inverse of temperature (Arrhenius plot) for different process of F6BBiOC8.

TABLE II

Dielectric relaxation parameters of 6F6BBiOC8.

	SmC* (102 °C)	
	MW	GM
$\Delta\varepsilon$	27.3 ± 2.76	21.91 ± 0.43
ν_R	(32.87 ± 4.57) Hz	(1674.78 ± 15.95) Hz
α	0.29 ± 0.03	0.12 ± 0.01
$\varepsilon(\infty)$	3.90 ± 0.01	
σ	$(2.58 \pm 0.08) \times 10^{-8}$ S/m	
	SmC*_A (66 °C)	
	AFM1	AFM2
$\Delta\varepsilon$	2.21 ± 0.01	0.10 ± 0.01
ν_R	(399.01 ± 3.97) Hz	(146.53 ± 18.77) kHz
α	0.16 ± 0.01	0.00
$\varepsilon(\infty)$	3.97 ± 0.01	
σ	$(2.57 \pm 0.02) \times 10^{-9}$ S/m	

antiferroelectric phase the MW relaxation is not present. It is mainly due to a considerable reduction of conductivity. As seen, the dielectric parameters of MW relaxation and GM (Fig. 7) are not strongly temperature dependent.

3.4. Bias field influence

After applying the bias field of 20 V/5 μm the low frequency MW relaxation disappears (Fig. 8b) whereas the

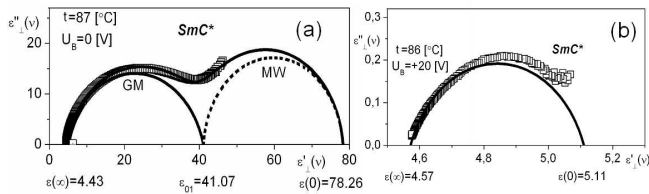


Fig. 8. Dielectric spectrum measured in the SmC* phase of m4F6BBiOC8 without (a) and with bias voltage (b).

GM is suppressed. The process which survives application of the strong electric field is a non-Arrhenius process.

Figure 8 illustrates how the bias field influences the dielectric properties of real ferroelectric liquid crystals.

4. Conclusion

- Temperature ranges of SmC* phase and SmC*_A phases depend on the structure of fluorinated tail. The SmC*_A was detected dielectrically only for the compound having the longest molecule 6F6BBiOC8, but the temperature range of this phase is rather narrow.
- Spontaneous polarization P_s does not depend distinctly on the molecular chain length.
- In the SmC* two collective modes (GM and MW) were found for all substances studied whereas in the antiferroelectric phase two processes were observed: AFM1 and AFM2 — one of them might be a collective mode (NCM) and the other one — a molecular process.
- The antiferroelectric SmC*_A phase displays much smaller conductivity and does not show MW relaxation. These two factors are important for applications.

References

- [1] R. Dąbrowski, *Ferroelectrics* **243**, 1 (2000).
- [2] A. Mikułko, M. Marzec, S. Wróbel, R. Dąbrowski, *Opto-Electron. Rev.* **14**, 319 (2006).
- [3] M. Marzec, A. Mikułko, S. Wróbel, A. Szymańska, R. Dąbrowski, *Mol. Cryst. Liq. Cryst.* **480**, 140 (2008).
- [4] A. Mikułko, M. Marzec, M.D. Ossowska-Chruściel, J. Chruściel, S. Wróbel, *Ferroelectrics* **343**, 209 (2006).
- [5] S. Wróbel, W. Haase, A. Fąfara, M. Marzec, in: *Relaxation Phenomena, Liquid Crystals, Magnetic Systems, Polymers, High-T_c Superconductors, Metallic Glasses* Eds. S. Wróbel, W. Haase, Springer-Verlag, Heidelberg 2003, Ch. 5.11.